

GA-A25414

MODELING OF LARGE ELM SUPPRESSION FOR HIGH CONFINEMENT PLASMA IN DIII-D

by
L.W. YAN and T.E. EVANS

JUNE 2006



DISCLAIMER

This report was prepared as an account of work sponsored by an agency of the United States Government. Neither the United States Government nor any agency thereof, nor any of their employees, makes any warranty, express or implied, or assumes any legal liability or responsibility for the accuracy, completeness, or usefulness of any information, apparatus, product, or process disclosed, or represents that its use would not infringe privately owned rights. Reference herein to any specific commercial product, process, or service by trade name, trademark, manufacturer, or otherwise, does not necessarily constitute or imply its endorsement, recommendation, or favoring by the United States Government or any agency thereof. The views and opinions of authors expressed herein do not necessarily state or reflect those of the United States Government or any agency thereof.

GA-A25414

MODELING OF LARGE ELM SUPPRESSION FOR HIGH CONFINEMENT PLASMA IN DIII-D

by
L.W. YAN* and T.E. EVANS

This is a preprint of a paper to be presented at
the 17th International Conference on Plasma
Surface Interactions in Controlled Fusion
Devices, Hefei, China, May 22–26, 2006 and to be
printed in the Proceedings

*Southwestern Institute of Physics, Chengdu, Sichuan, China

**Work supported by
the U.S. Department of Energy
under DE-FC02-04ER54698**

**GENERAL ATOMICS PROJECT 30200
JUNE 2006**



ABSTRACT

A 3-D field line integration code (TRIP3D) is used to trace stochastic field lines in the edge of DIII-D plasmas in which edge localized modes (ELMs) are suppressed by resonant magnetic perturbations (RMPs). In these experiments normalized RMPs of 2.6×10^{-4} on the 95% flux surface produce complete ELM suppression, while plasma confinement stays high. The calculated particle diffusion coefficients produced by stochastic magnetic field on 95% flux surface are $0.29 \text{ m}^2/\text{s}$ with full ELM suppression and $0.046 \text{ m}^2/\text{s}$ in a reference discharge without the RMPs and with no ELM suppression. The corresponding collisionless electron conductivities in these two discharges are $6.7 \text{ m}^2/\text{s}$ and $1.25 \text{ m}^2/\text{s}$. The thermal conductivity estimated from energy confinement time is $2.4 \text{ m}^2/\text{s}$ with and without ELM suppression. TRIP3D modeling indicates that the stochastic magnetic field inside 95% flux surface is rather important for enhancing edge transport and suppressing large ELMs.

1. INTRODUCTION

H-mode discharges with high edge pressure gradients are expected to be required for the economic feasibility of future fusion reactors. However, the high edge pressure gradients easily produce an ELM instability [1], which expels large heat and particle loading to the divertor targets. These ELMs limit the core plasma performance and reduce the lifetime of divertor target plates. The transport of heat and particles outward across the plasma boundary is useful to control density and impurity profiles for steady-state, high-performance operations. Consequently, any technique to eliminate or mitigate large fast ELM impulses must replace the transient heat and particle transport with another quasi-steady transport process. Such a technique is high priority for a burning plasma device such as ITER [2].

Recently, several methods have been found to avoid large ELMs. The quiescent H-mode (QH-mode) is a type of high performance discharge, without large ELMs discovered on DIII-D and reproduced in other devices [3]. The enhanced D_α (EDA) H-mode, obtained in Alcator C-Mod, depends on a quasi-coherent MHD mode near the separatrix for particle control [4]. Another H-mode scenario without large ELMs is high recycling steady (HRS) H-mode observed in JFT-2M [5]. H-modes with small ELMs have been reported in high triangularity plasmas in JT-60U [6]. Recent ELM suppression experiments in DIII-D indicate that static resonant magnetic perturbations can effectively decrease or eliminate large, fast ELMs in high confinement plasmas without degrading the performance [7,8]. This suppression depends on magnetic perturbation amplitude, safety factor, heating power and plasma density.

2. EXPERIMENTAL RESULTS OF LARGE ELM SUPPRESSION

Steady-state H-mode plasmas without large ELMs have been achieved in the DIII-D tokamak by applying small resonant magnetic field perturbations [8]. In these experiments, a normalized radial magnetic perturbation of 2.6×10^{-4} on the 95% flux surface produces complete ELM suppression, while plasma confinement stays high. The typical discharge parameters used to obtain complete ELM suppression are given for DIII-D discharge 123301 with an $n = 3$ I-coil perturbation along with a reference to an I-coil case without ELM suppression in Table 1. In discharge 123301 both the single turn I-coil, located inside the vacuum vessel, and the four-turn C-coil located outside the vacuum vessel are used to completely eliminate ELMs, while in discharge 123302 with the C-coil but without the I-coil the ELMs are not suppressed. An increase in the divertor CIII emission in discharge 123301 suggests that particles from inside the magnetic separatrix directly reach divertor plates across a stochastic boundary with the I-coil RMP. This increase in CIII is not seen in discharge 123302 without the I-coil RMP. The H-factor and normalized beta increase slightly in ELM suppressed discharges compared to those without ELM suppression. Here, we model the magnetic field line structure of discharge 123301 and 123302 and compare the changes due to the I-coil RMP.

Table 1
Key Plasma and Perturbation Coil Parameters used in
DIII-D Discharges 123301 and 123302 at 3000 ms

Discharge number (123-)	301	302
Major radius (m)	1.65	1.65
Minor radius (m)	0.60	0.60
Toroidal field (T)	-2.0	-2.0
Plasma current (MA)	1.5	1.5
Safety factor at $\psi_N = 0.95$	3.7	3.7
NBI Power (MW)	8.0	8.0
C-coil current (kAt)	12.0	12.0
I-coil ($n = 3$) current (kAt)	3.3	0.0

3. THE MODELING OF STOCHASTIC FIELD TRANSPORT

A three-dimensional field line integration code, TRIP3D, was developed to model stochastic magnetic boundaries in poloidally diverted tokamaks [9]. In TRIP3D, the unperturbed magnetic field (B_R, B_ϕ, B_Z) at each point is provided by the EFIT code [10]. The perturbed field (b_R, b_ϕ, b_Z), produced by I-coil and C-coil currents, is calculated for each integration step and added to the unperturbed axisymmetric EFIT field. The code integrates a set of first-order cylindrical (R, ϕ, Z) magnetic differential equations given as

$$\frac{\partial R}{\partial \phi} = \frac{R(B_R + b_R)}{B_\phi + b_\phi}, \quad \frac{\partial Z}{\partial \phi} = \frac{R(B_Z + b_Z)}{B_\phi + b_\phi}. \quad (1)$$

The diffusion coefficient that can be calculated in TRIP3D and is representative of the stochasticity of a field line is defined as, $D_{st} = \delta r^2 / 2L$, where δr is the radial random step and L is the field line length. Here, L is taken in the limit of 200 toroidal revolutions or when the field line hits a material surface such as a divertor target plate. Recently, TRIP3D was modified to calculate the minor radius at different poloidal angles on the same unperturbed flux surface in elongated DIII-D plasmas. In this case, the radial step is replaced by the normalized magnetic perturbation in the calculation of the diffusion coefficient $\langle D_{st}^\psi \rangle = \frac{1}{M} \sum_{i=1}^M \delta \psi_i^2 / 2L_i$, where $\delta \psi_i$ is the flux step and M is the number of field lines included in the calculation on each flux surface. The two diffusion coefficients are related by $\langle D_{st} \rangle = C^2 r^2 \langle D_{st}^\psi \rangle / 4 \psi_i^2$. The coordinate conversion coefficient is $C = 1.03 - 1.27$ for the DIII-D discharges. $C = 1.25$ is a reasonable approximation for edge plasma. The radial particle diffusion coefficient is calculated using $D_m = \langle D_{st} \rangle \times C_s$, where $C_s = \sqrt{(T_e + T_i) / m_i}$ is the ion acoustic speed. In contrast, collisionless electron conductivity is defined as [11], $\chi_e = \langle D_{st} \rangle \times v_{Te}$, where $v_{Te} = \sqrt{T_e / m_e}$ is thermal electron speed.

4. CALCULATION RESULTS FOR ELM SUPPRESSION IN DIII-D

Figure 1 shows a Poincaré plot of the field line positions for normalized magnetic flux versus poloidal angle for shot 123301 at $t = 3.0$ s with complete ELM suppression. Here, seventy-two uniformly distributed field lines are followed on each flux surface starting at $\psi_N = 0.7$ and ending at $\psi_N = 1.0$ with the step of $\Delta\psi_N = 0.05$. Each field line is preset for a maximum of 200 toroidal revolutions that results in a maximum length of about 2000 m or roughly of order a collisional electron mean free path (L_c). For example, using $T_{e,95} = 1.2$ keV, $n_{e,95} = 1.3 \times 10^{19}$ m⁻³, we find $L_{c,95} = 942$ m at $\psi_N = 0.95$. The large $m/n = 2/1$ magnetic island seen at $\psi_N = 0.67$ has a width $\Delta\psi_N = 0.06$ and results from the C-coil which is configured to correct $n = 1$ field-errors in these experiments. The C-coil also produces an $m/n = 3/1$ island chain on the $\psi_N = 0.88$ surface with a width $\Delta\psi_N = 0.025$. It should be noted that there are also small islands between $\psi_N = 0.78$ and $\psi_N = 0.84$ produced by the $n = 3$ I-coil perturbations and field-errors from various sources. Field line dots occupy almost entire space except island regions even with the step of $\Delta\psi_N = 0.05$. The combined I-coil, C-coil and field-error perturbations produce a relatively strong stochastic boundary region in these plasmas and field lines begin to connect to the divertor targets in less than 200 revolutions once $\psi_N > 0.80$. This relatively strong degree of stochasticity also reduces the islands widths. All of the open field lines eventually hit the lower divertor in this lower single null (LSN) discharge. There are 4 stripe-like features

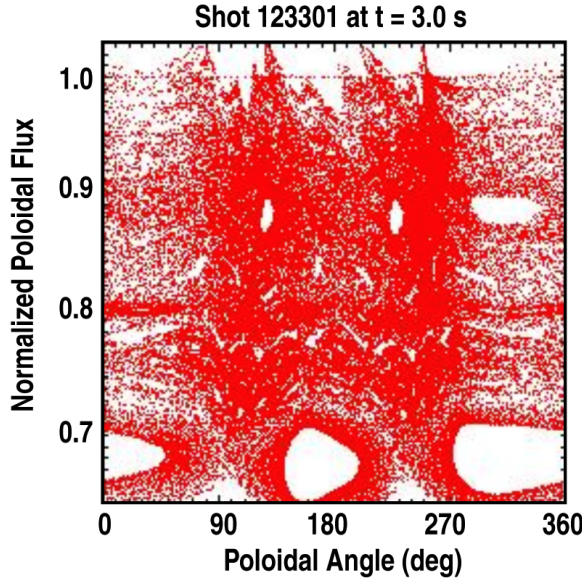


Fig. 1. Poincaré plot of the field line positions for normalized magnetic flux versus poloidal angle in shot 123301 at $t = 3$ s with complete ELM suppression.

between 80 deg and 250 deg on the top near $\psi_N = 1.0$, which are consistent with the Hamiltonian structure of the system and a splitting of the separatrix into two invariant manifolds [12,13] (only one of which is seen because the field lines in this figure are all integrated in one direction from the starting point). Here, the edge safety factor is larger than 4 and coincides with the 4 stripe-like features defined by one of the invariant manifolds. Note that the density of field line intersections with the Poincaré plane is higher between 90 deg and 270 deg indicating that the field lines spend more time in the HFS than in the LFS. In discharge 123302, with the C-coil and field-errors but no I-coil, the stochasticity is significantly weaker and wider magnetic islands are observed.

Figure 2 shows the distribution of radial flux steps $\delta\psi_N$ found after integrating through a toroidal angle $\Delta\phi = 90^\circ$ in the I-coil on discharge at time $t = 3.0$ s starting from $\psi_N = 0.95$. The maximum step with the I-coil is $\delta\psi_N = 2.4\%$, which often appears just before the field lines hit the divertor targets. Most steps are $\delta\psi_N \leq 0.29\%$. The relatively good symmetry of distribution about $\delta\psi_N = 0$ indicates that many toroidal revolutions of the field lines are needed before being lost to the divertor. The maximum count is 8451 with $\delta\psi_N = -0.058\%$. The wings of the distribution are dominated by near field interactions as the field lines pass through regions close to the I-coil. Large magnetic islands produce an additional degree of complexity in the distribution since the trajectories can become very chaotic near the islands.

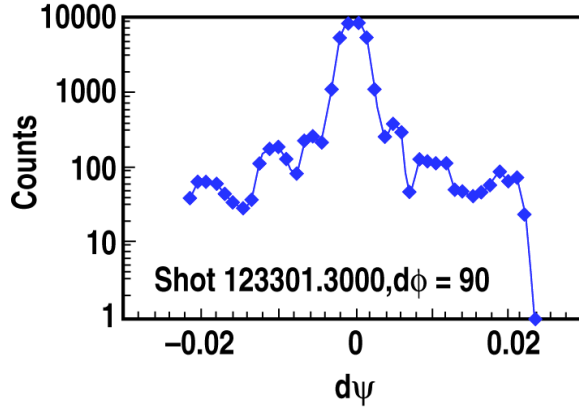


Fig. 2. Counts versus the flux steps within toroidal angle of 90 deg for shot 123301 at $t = 3.0$ s.

The maximum flux step size ($\delta\psi_N$) with the I-coil off decreases to $\delta\psi_N = 1.65\%$, and is dominated by the $m/n = 4/1$ magnetic island. The step size difference of short, $\Delta\phi = 90^\circ$, path integrals with (discharge 123301) or without (discharge 123302) ELM suppressions is not very large. Calculations of the field line properties using long path integrals ($\Delta\phi \gg 90^\circ$) is expected to be related to a global magnetic diffusion coefficient of the system since local effects are reduced.

Figure 3 shows the stochastic magnetic diffusion coefficient $\langle D_{st} \rangle$ versus normalized flux for a discharge with the I-coil (upper) and without (lower). Here, 180 field lines are traced on each flux surface and the flux step $\Delta\psi_N$ between each surface is 0.01. As seen in

Fig. 3, the edge magnetic diffusion coefficient with the I-coil tends to decrease with normalized magnetic flux for $\psi_N > 0.84$. The stochastic magnetic field line diffusion coefficient at $\psi_N = 0.95$ is $\langle D_{st} \rangle = 4.6 \times 10^{-7}$ m. Based on this, the radial particle diffusion coefficient is $D_m = 0.29$ m²/s using ion acoustic speed $C_s = 6.3 \times 10^5$ m/s by $T_{e,95} = 1.2$ keV and $T_{i,95} = 3$ keV, while collisionless electron conductivity is $\chi_e = 6.7$ m²/s. The energy confinement time in this discharge, calculated using a diamagnetic energy of 1.176 MJ and a neutral beam power of $P_{NBI} = 8$ MW, is $\tau_E = 147$ ms. The thermal conductivity is then $\chi_{exp} = a^2 / \tau_E = 2.4$ m²/s, which is smaller than 6.7 m²/s. Therefore, the edge diffusion appears to be dominated by stochastic magnetic field after large ELM suppression. Results from TRIP3D also show that the field line length abruptly drops in edge region because of field lines lost on divertor targets, with lengths of 1976 m at $\psi_N = 0.7$, 1124 m at $\psi_N = 0.95$ and 497 m at $\psi_N = 0.99$.

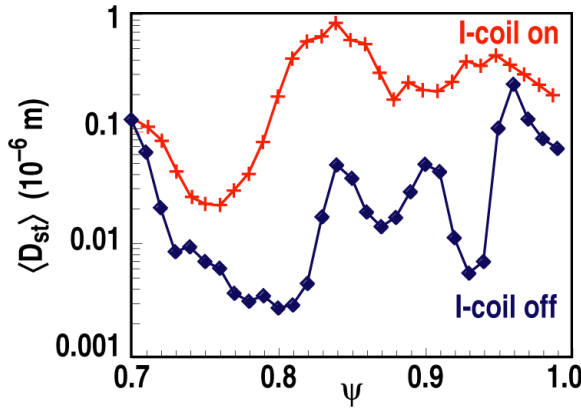


Fig. 3. Magnetic diffusion coefficient versus normalized flux for shot 123301 and 123302.

The magnetic diffusion coefficient in the discharge without the I-coil perturbation field is well below that in the discharge with the I-coil perturbation field. Here, the particle radial diffusion coefficient is $D_m = 0.046$ m²/s using $C_s = 4.6 \times 10^5$ m/s by $T_{e,95} = 0.9$ keV and $T_{i,95} = 1.3$ keV, while collisionless electron conductivity is $\chi_e = 1.25$ m²/s. This level of stochasticity is apparently insufficient to suppress the large ELMs.

Figure 4 shows the radial variation in field line hit points for discharge 123301 with the I-coil currents versus toroidal angle on the lower divertor targets which are located near poloidal angle 250 deg in these LSN diverted discharges, as shown in Fig. 1. The hit profile is asymmetric along toroidal direction dependent on the asymmetry of I-coil currents. The hit width is 1.5 – 7.0 cm and there are three clear stripes indicating that the toroidal mode of I-coil currents ($n = 3$) is determining the structure of the field line hit pattern on the divertor targets. This pattern is consistent with lobes from an invariant manifold intersecting the divertor targets when the separatrix is split by the $n = 3$ I-coil perturbation [13]. The maximum width of the field line hit pattern in the discharge without the I-coil drops to 4 cm and the pattern changes to that of a single strips. In addition, fewer field lines hit the divertor

plates in discharge without the I-coil because of the weaker stochastic field produced by DIII-D field errors. The broader radial profile of hit points in the discharge with the I-coil is expected to spread the heat load on the divertor but, at the same time, more field lines from the region of the pedestal plasma hit the divertor targets. Images of the divertor using IR data for the discharge modeled here do not show evidence of heat flux spreading during the I-coil perturbation, although in other discharges using the I-coil, a splitting of the heat flux is observed [12].

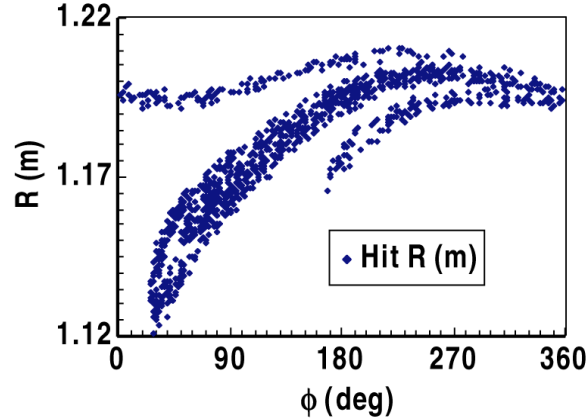


Fig. 4. Major radius of hit points versus toroidal angle for shot 123301.

5. CONCLUSIONS

Large ELMs have been completely suppressed in DIII-D using stochastic magnetic boundary provided by I-coil and C-coil currents. The radial magnetic perturbation is increased in discharges with ELM suppression, while plasma confinement stays high. The 3-D TRIP3D modeling indicates that the stochastic magnetic field inside normalized flux surface of $\psi_N = 0.95$ may be important for enhancing edge transport and suppressing large ELMs. The radial particle diffusion coefficients produced by stochastic field on flux surface $\psi_N = 0.95$ are $0.29 \text{ m}^2/\text{s}$ with full ELM suppression and $0.046 \text{ m}^2/\text{s}$ without ELM suppression, the corresponding collisionless electron conductivities are $6.7 \text{ m}^2/\text{s}$ and $1.25 \text{ m}^2/\text{s}$. The global thermal conductivity estimated from energy confinement time is $2.45 \text{ m}^2/\text{s}$ with and without ELM suppression. The modeling results show that the stochastic region is making a significant contribution to the edge diffusion in discharges with large ELM suppression. Modeling indicates that the field line hit pattern on the divertor target plates in discharges with ELM suppression have an $n = 3$ toroidal asymmetry due to the $n = 3$ I-coil perturbation field and a radial width of $1.5 - 7.0 \text{ cm}$.

REFERENCES

- [1] A. Loarte, M. Becoulet, G. Saibene, et al. *Plasma Phys. and Control. Fusion* **44** (2002) 1815.
- [2] ITER Physics Basis, *Nucl. Fusion* **39** (1999) 2137.
- [3] C.M. Greenfield, K.H., Burrell, J.C. DeBoo, et al. *Phys. Rev. Lett.* **86** (2001) 4544.
- [4] J.E. Rice, P.T. Bonoli, E.S. Marmar, et al. *Nucl. Fusion* **42** (2002) 510.
- [5] K. Kamiya, H. Kimura, H. Ugawa, et al. *Nucl. Fusion* **43** (2003) 1214.
- [6] Y. Kamada, Y. Oikawa, L. Lao, et al. *Plasma Phys. Control. Fusion* **42** (2000) A247.
- [7] T.E. Evans, R.A. Moyer, P.R. Thomas, et al. *Phys. Rev. Lett.* **92** (2004) 2350003-1.
- [8] K.H. Burrell, T.E. Evans, E.J. Doyle, et al., *Plasma Phys. Control. Fusion* **47** (2005) B37-B52.
- [9] T.E. Evans, R.A. Moyer and P. Monat *Phys. Plasmas* **9** (2002) 4957.
- [10] L. Lao, R.H. St. John, R.D. Stambaugh, et al. *Nucl. Fusion* **25** (1985) 1611.
- [11] A.B. Rechester, M.N. Rosenbluth, *Phys. Rev. Lett.* **40** (1978) 38.
- [12] T.E. Evans, R.K. W. Roeder, J.A. Carter, et al., *J. Phys.: Conf. Ser.* **7** (2005) 174.
- [13] R.K. W. Roeder, B.I. Rapoport and T.E. Evans, *Phys. Plasmas* **10** (2003) 3796.

ACKNOWLEDGMENTS

This work was supported in part by the U.S. Department of Energy under DE-FC02-04ER54698, DE-AC02-76CH03073 and DE-AC05-00OR22725 and by the Chinese Ministry of Science and Technology under 001CB710904 through the fusion collaboration between China and USA on fluid plasma simulation. We would like to thank Dr. C. Wong of General Atomics for arranging the collaboration.